



# Contrast-Enhanced Magnetic Resonance Imaging Suggested a Possibility of Transvenous Embolization in the Superior Petrosal Sinus Dural Arteriovenous Fistula: A Case Report

Masahiro Nishihori,<sup>1</sup> Takashi Izumi,<sup>1</sup> Tetsuya Tsukada,<sup>1</sup> Yutaka Kato,<sup>2</sup> Kenji Uda,<sup>1</sup> Kinya Yokoyama,<sup>1</sup> Yoshio Araki,<sup>1</sup> and Ryuta Saito<sup>1</sup>

**Objective:** Superior petrosal sinus dural arteriovenous fistula (SPS-DAVF) is a rare subtype of intracranial DAVF that sometimes leads to hemorrhagic symptoms following deep venous drainage. Here we report the case of SPS-DAVF with retrograde venous reflux to the cerebellar vein. Preoperative contrast-enhanced MRI was a decisive factor in a safe and effective treatment.

**Case Presentation:** A 37-year-old woman was referred to our hospital with abnormal MRI findings, which was performed when she had a mild headache during her check-up. DSA revealed left-sided SPS-DAVF, which was diagnosed as Cognard type IIb. Both CTA and DSA could not detect the whole SPS but only the shunt pouch. Using contrast-enhanced MRI, we were able to visualize the presence of the SPS and its continuity within the shunt pouch. 3D-T1 turbo spin echo (SPACE) showed a low-intensity area in the SPS, which was not seen in the 3D-T1 fast field echo (FFE). During the procedure, there was a point where it was difficult to advance the microcatheter, which coincided with the low-intensity area. We achieved effective transvenous embolization from the occluded venous access by devising a surgical technique.

**Conclusion:** In addition to the contrast-enhanced 3D-T1 FFE, 3D-T1 SPACE might provide beneficial information for endovascular therapy in the evaluation of venous sinuses, which could not be detected by standard examinations.

**Keywords** ▶ dural arteriovenous fistula, transvenous embolization, contrast-enhanced magnetic resonance imaging, superior petrosal sinus

## Introduction

Superior petrosal sinus dural arteriovenous fistula (SPS-DAVF) is an extremely rare entity, accounting for 0.5%–4.5% of all intracranial dural AVFs.<sup>1,2)</sup> A previous study

reported that the SPS is not visualized using DSA in only 1.2% of patients and is visualized using carotid or vertebral angiography for a majority of patients.<sup>3)</sup> However, reports on endovascular treatment (EVT) for SPS-DAVF are limited, in which successful EVTs were conducted when arterial feeders are large enough or the shunt is adjacent to the patent venous sinus.<sup>4,5)</sup> One of the reasons for this is that there might be potential cases where EVT has been deemed impossible because the occluded veins cannot be visualized by conventional examinations alone. Hosoo et al. reported the method to visualize occluded dural sinus using contrast-enhanced MRI.<sup>6)</sup> Details of the venous sinus were delineated by adding high-resolution contrast-enhanced 3D turbo spin echo (TSE) MRI using their method. Here, we describe a case of SPS-DVAF, in which preoperative contrast-enhanced MRI distinctly made visibly occluded venous sinus not visualized by other modalities, thus resulting in definitive transvenous embolization (TVE).

<sup>1</sup>Department of Neurosurgery, Nagoya University Graduate School of Medicine, Nagoya, Aichi, Japan

<sup>2</sup>Department of Radiological Technology, Nagoya University Hospital, Nagoya, Aichi, Japan

Received: March 3, 2021; Accepted: June 9, 2021

Corresponding author: Masahiro Nishihori. Department of Neurosurgery, Nagoya University of Graduate School of Medicine, 65, Tsurumaicho, Showa-ku, Nagoya, Aichi 466-8550, Japan  
Email: nishihori@med.nagoya-u.ac.jp



This work is licensed under a Creative Commons Attribution-NonCommercial-NoDerivatives International License.

©2022 The Japanese Society for Neuroendovascular Therapy

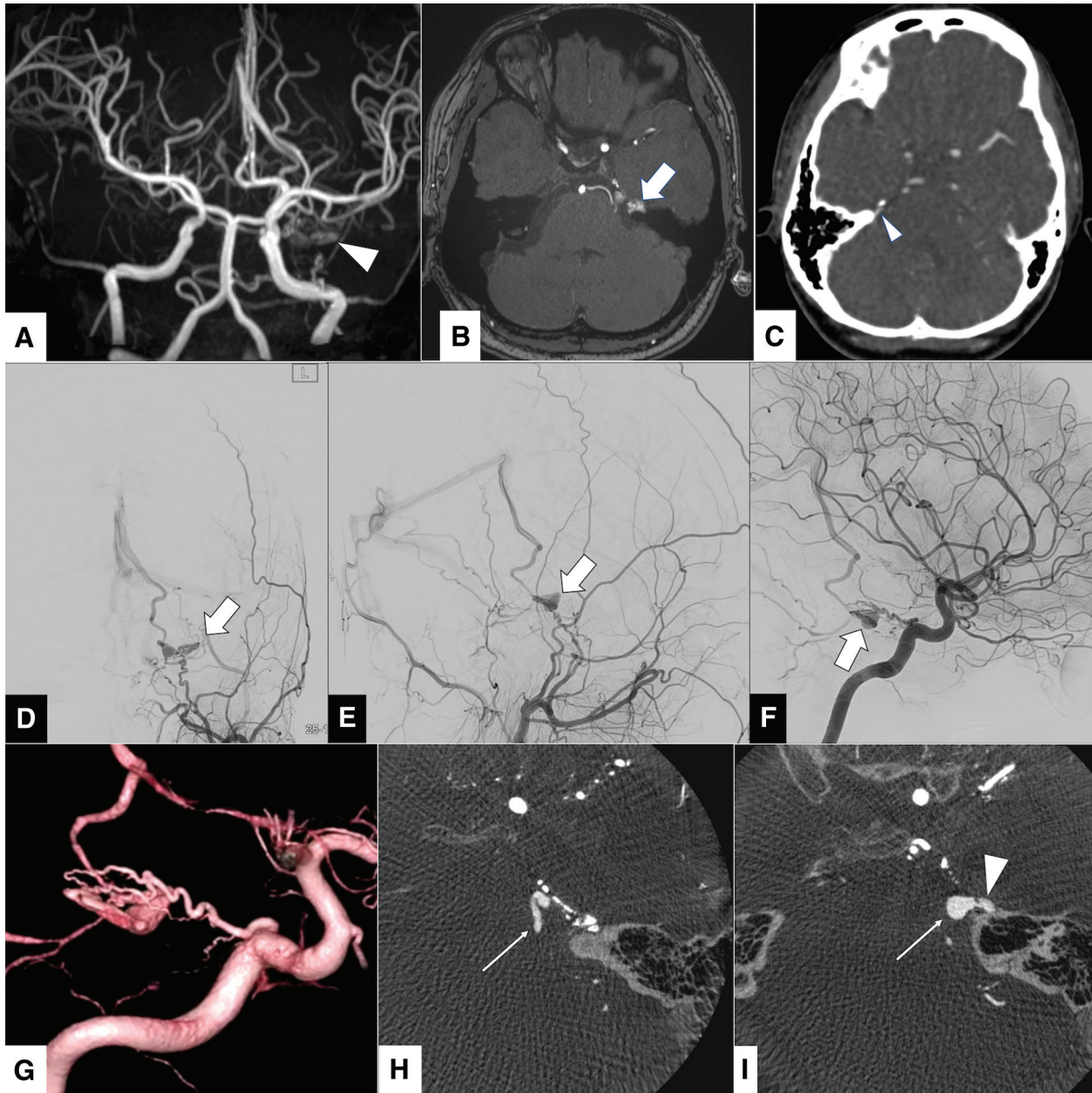


**Fig. 1** Preoperative images. (A) Maximum intensity projection image of MRA is shown. The arrowhead shows an abnormal vascular signal. (B) The source image of the MRA. Similarly, the arrow indicates an abnormal vascular signal at the tip of the petrosal bone. (C) An axial image of CTA. This image revealed no ipsilateral SPS. The thin arrowhead shows a portion of the contralateral SPS. (D–F) Preoperative DSA images. (D and E) are left external carotid

angiography, and (F) is left ICAG. White arrows indicate abnormal shunt and shunt pouch (D: anteroposterior view, E and F: lateral view). (G) is a volume rendering technique 3DRA image of the left ICAG, with source images in (H) and (I). In those source images, the thin arrows indicate the drainer side including varix, and the arrowhead indicates the shunt pouch. 3DRA: 3D rotation angiography; ICAG: internal carotid angiography; SPS: superior petrosal sinus

## Case Presentation

A 37-year-old woman was referred to our hospital with abnormal MRI findings performed during her mild headache check-up. The patient had no pertinent medical history. During hospitalization, the patient was neurologically intact, with a mild headache. MRI showed neither parenchymal

hemorrhage nor edema. MRA and CTA revealed abnormal AV shunt around the left SPS (Fig. 1A–1C); moreover, DSA was performed (Fig. 1D–1F). All feeders are left-sided, located at the meningo-hypophyseal trunk (MHT), accessory meningeal artery, and a petrosal branch of the middle meningeal artery. The shunt pouch was located at the dura mater of the petrosal ridge, and the whole or segments

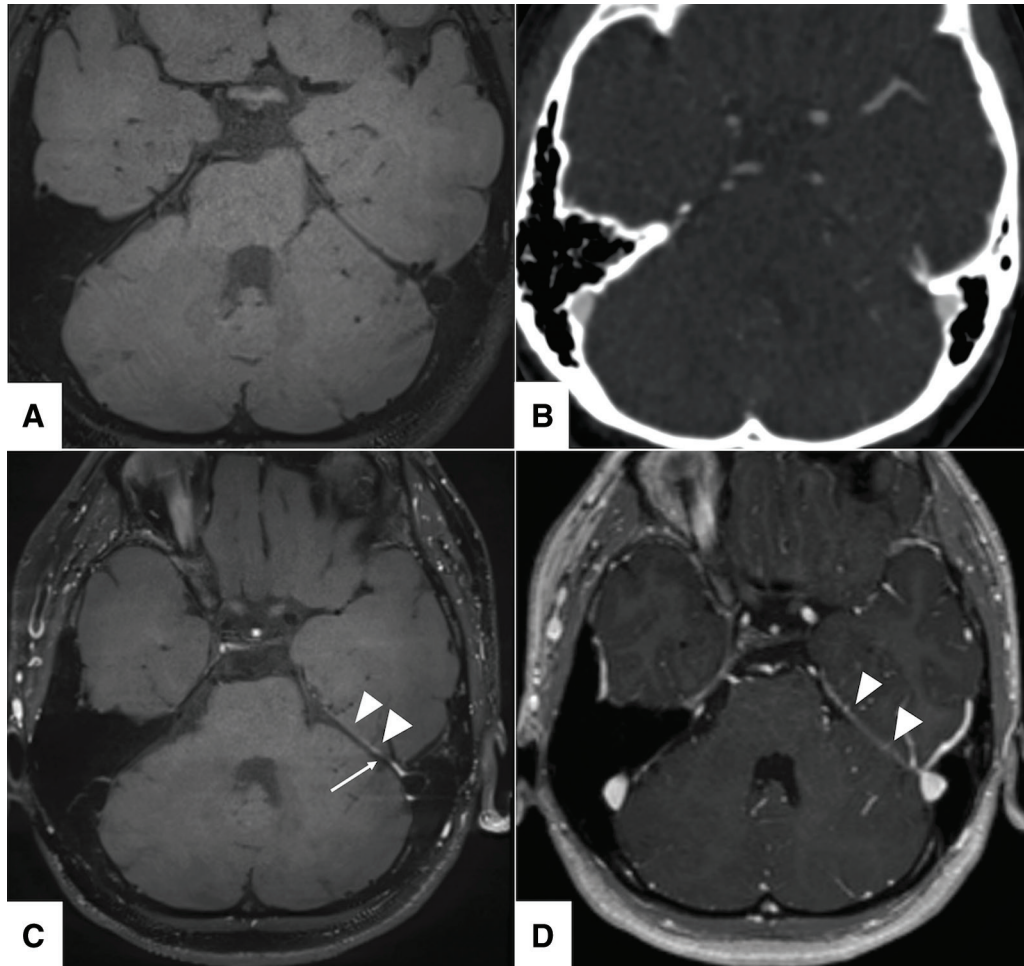


**Fig. 2** Comparison of contrast-enhanced MRI and CT. (A) A simple 3D-T1 TSE (SPACE), (B) an axial image of CTA, and (C and D) a contrast-enhanced MRI at the same slice level. (C) is 3D-T1 SPACE imaging, and (D) is 3D-T1 FFE. The arrowheads show enhanced SPS, and the thin arrow shows the area of decreased signal in contrast-enhanced 3D-T1 SPACE images. FFE: fast field echo; SPACE: sampling perfection with application optimized contrasts using different flip angle evolutions; SPS: superior petrosal sinus; TSE: turbo spin echo

of SPS itself were not depicted. A retrograde cortical venous drainage was reported that flowed out to ipsilateral cerebellar veins through the left petrosal vein. In terms of drainers, the proximal side was the left petrosal vein, and the lateral mesencephalic vein, the basal vein of Rosenthal, interhemispheric vein, and vein of the lateral recess of the fourth ventricle were drainers of the distal side. The petrosal vein was dilated to form a varix, as diagnosed by Cognard type IIb DAVF. The volume rendering images and source images of the 3D rotation angiography (3DRA) revealed details of vascular architecture (**Fig. 1G–1I**). In general, tentorial dural AVF including SPS has been known to cause hemorrhage changes and should be treated because of their high Cognard grades.<sup>1,7,8</sup> It is also known that >90% of patients have been reported to become symptomatic after a long-term observation.<sup>7,9</sup> Therefore, we believed that surgical treatment was indicated even if the patient was asymptomatic.

After providing sufficient informed consent, the patient hoped to undergo some treatment. A skull-based surgeon was consulted because the anterior petrosal or retrosigmoid approach would be necessary if a craniotomy would be performed. However, the protuberant operculum of petrous bone possibly obstructed the visual field and therefore the surgical difficulty was high, in addition to high surgical invasion. Considering the EVT, transarterial embolization (TAE), using the liquid embolic material, is possible; however, concerns about the migration of cast into dangerous anastomosis to the vasa nervorum might cause neurological complications. However, if TVE would be possible, the treatment risk was extremely low, and thus, it seemed to be a safe and definitive treatment. Therefore, to explore the possibility of less-invasive EVT, contrast-enhanced MRI was performed to evaluate the patency of the SPS and the positional relationship between the SPS and shunt.

### Contrast-enhanced MRI

**Figure 2** shows each CTA and MRI compared side by side at the same level. In addition to the simple T1-weighted image (T1WI) (**Fig. 2A**), contrast-enhanced 3D-T1 fast field echo (FFE) and 3D-T1 TSE MRI (sampling perfection with application optimized contrasts using different flip angle evolutions; SPACE) were performed (**Fig. 2C** and **2D**). In simple T1WI, SPS was not visualized; however, contrast-enhanced 3D-T1WI clearly demonstrated SPS (**Fig. 2C** and **2D**). The whole SPS was visualized in 3D-T1 FFE (**Fig. 2D**), whereas fat-suppressed SPACE MRI demonstrated a low-intensity area in the middle of the SPS (**Fig. 2C**). Since 3D-TSE MRI (SPACE) is black blood imaging, the flow void showed low-intensity around shunt, while 3D-T1 FFE shows clear connectivity among SPS, shunt pouch, and drainer. If catheterization would be achieved into this SPS, TVE was considered sufficiently feasible.

### Transvenous Embolization

Endovascular procedures were performed under local anesthesia and mild conscious sedation. After obtaining the percutaneous femoral arterial and venous access, patients were heparinized based on their body weight (60–100 IU/kg) to maintain an activated clotting time between 200 and 300. A 6-F shuttle sheath (Cook Medical, Bloomington, IN, USA) was placed in the right internal jugular vein. A 4-F diagnostic catheter was placed in the left internal carotid artery for angiography. A 6-F FUBUKI (Asahi Intecc, Aichi, Japan) and 3.4-F TACTICS 130 cm (Technocrat corporation, Aichi, Japan) were coaxially inserted into the right transverse sinus (TS). This intermediate catheter TACTICS (Technocrat Corporation) was advanced to the vicinity of the SPS orifice to assist the pushability of the microcatheter. Since the positional relationship between the TS and SPS was known from the preoperative contrast-enhanced MRI, we explored the spot where the microguidewire tip would penetrate using the CHIKAI 0.014 microguidewire (Asahi Intecc). Headway 17 (Microvention, Aliso Viejo, CA, USA) was advanced to the place where the guidewire had entered (**Fig. 3A**). Then, microangiography revealed a luminal structure that appeared to be SPS (**Fig. 3B**). While the microguidewire advanced relatively easily, the following microcatheter did not advance from a certain point; therefore, a flexible part was inserted at the tip of the microguidewire for a long distance into the shunt pouch (**Fig. 3C**). It is well known that the proximal part of the microguidewire has a thick core wire. Therefore, this procedure provided good trackability of the

microcatheter when the proximal part of the guidewire advanced beyond the stenosis (**Fig. 3D**). Moreover, a cone beam CT confirmed that the tip of the microcatheter was located in the correct shunt pouch (**Fig. 3E** and **3F**). Therefore, 19 bare coils were packed back therefrom, thus achieving complete shunt disappearance (**Fig. 3G–3I**). The postoperative course was successful, and the patient was discharged without any problems. Her headache disappeared and no recurrence was observed for >3 years.

## Discussion

This case highlights the following: 1) a combination of contrast-enhanced MR with the venous sinus, which was initially thought to be occluded, allowed for a detailed understanding of the vascular morphology and resulted in safer surgery, and 2) contrast-enhanced 3D-T1 SPACE imaging, which is not commonly reported in vascular evaluation, was also important in the surgery. 3D-T1 contrast-enhanced MRI or magnetic resonance venography has been reported to be useful in evaluating routine venous anatomy in the skull base.<sup>10,11</sup> However, in patients with unidentified typical drainage, spatial resolution was reportedly insufficient to further delineate complex drainage structures.<sup>12</sup> **Figure 3** shows that the 3D-T1 contrast-enhanced MRI can show occluded or hairline lumens that are difficult to visualize with CTA or 3DRA. In addition to 3D-T1 FFE, which has already been reported to be useful,<sup>9</sup> high-resolution 3D-T1 TSE (SPACE) was used to evaluate the SPS detail before EVT. Compared to conventional 3D-T1 FFE, the SPACE method had a smaller voxel size, and thus a slightly lower contrast-to-noise ratio;<sup>13</sup> however, they had a higher spatial resolution. Furthermore, 3D-T1 SPACE has been reported to offer better visualization of the thrombus as compared to a standard MRI or MRA imaging for cerebral venous sinus thrombosis.<sup>14</sup>

Interpretation of an MRI was crucial in this case. The SPS which could not be demonstrated by DSA or CTA was initially thought to be occluded or hypoplastic. Simple T1WIs including 3D-T1 SPACE showed low signal, while 3D-T1 FFE showed that the entire SPS was well contrasted. Contrary to expectations, these results suggest that the SPS is neither hypoplastic nor occluded within the thrombus, but rather a condition with restricted blood flow. As mentioned above, immediately after entering the SPS, there was a certain point where the microcatheter was unable to advance, although the microguidewire passed

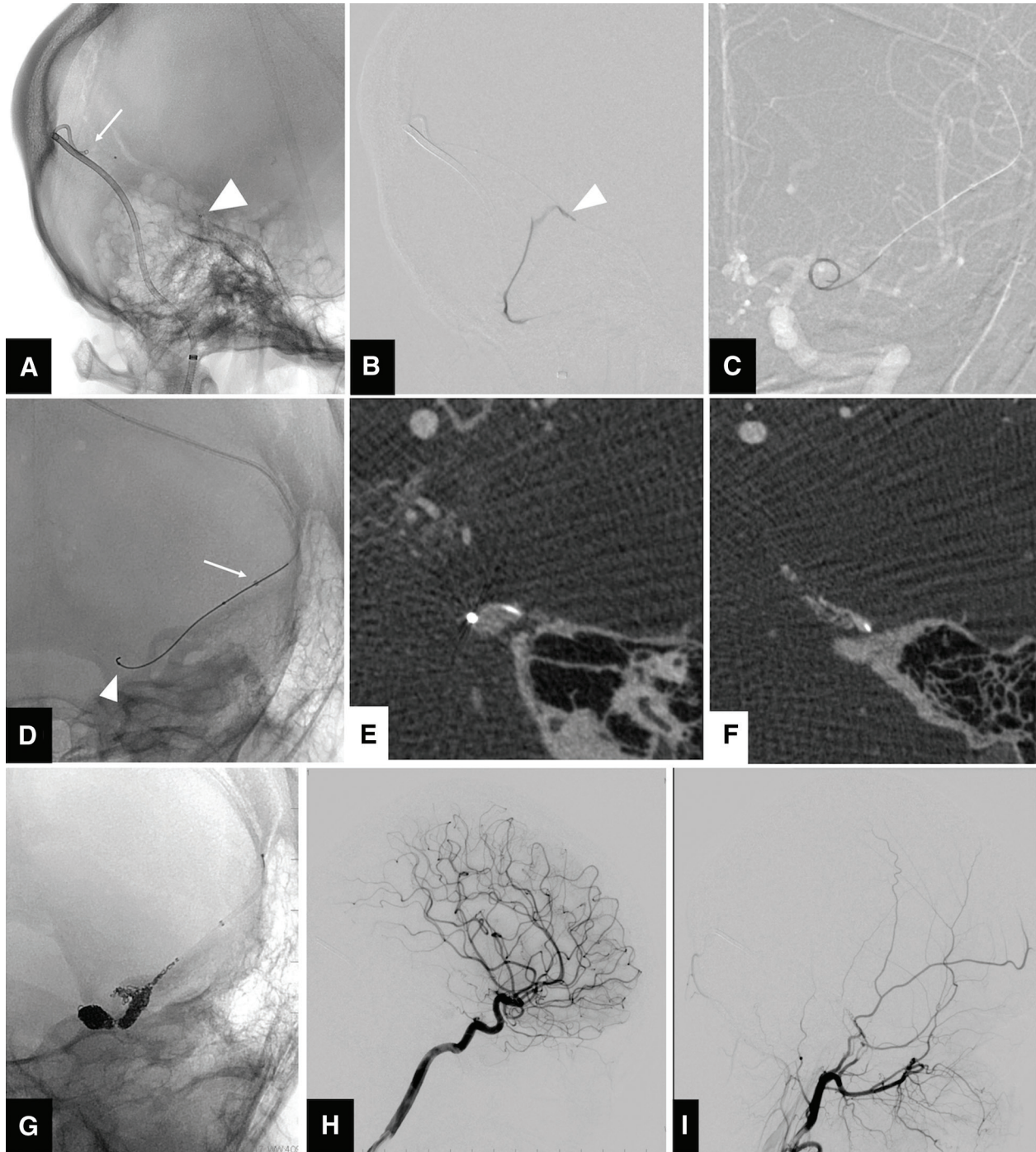


**Fig. 3** DSA images and CBCT images in TVE. **(A)** Lateral view of the DA image. The microcatheter was advanced toward the left SPS via contralateral TS. The thin arrow indicates the tip of the intermediate catheter, and the arrowhead indicates the microcatheter tip. **(B)** Lateral view of the micro angiography. The arrowhead indicates a part of the right SPS, and contrast medium is drained into the sigmoid sinus. **(C)** Fluoroscopic image under roadmap. The micro guidewire was successfully inserted into the shunt pouch or varix; however, the microcatheter would be stopped in the middle of the SPS due to catheter advancement resistance. **(D)** DA image showing the microcatheter advances into the SPS or shunt. The thin

arrow indicates the tip of the intermediate catheter that moved closer to the orifice of the SPS, and the arrowhead indicates the microcatheter tip entering into the SPS. **(E and F)** Sequential axial CBCT images showing that the microcatheter tip was guided into varix through the shunt. **(G)** DA image after coil embolization, showing that varix and shunt pouch were filled with coils. **(H and I)** Final lateral DSA images of the left ICAG and ECAG after TVE. The shunt has completely disappeared. CBCT: cone beam CT; DA: digital angiography; ECAG: external carotid angiography; ICAG: internal carotid angiography; SPS: superior petrosal sinus; TS: transverse sinus; TVE: transvenous embolization

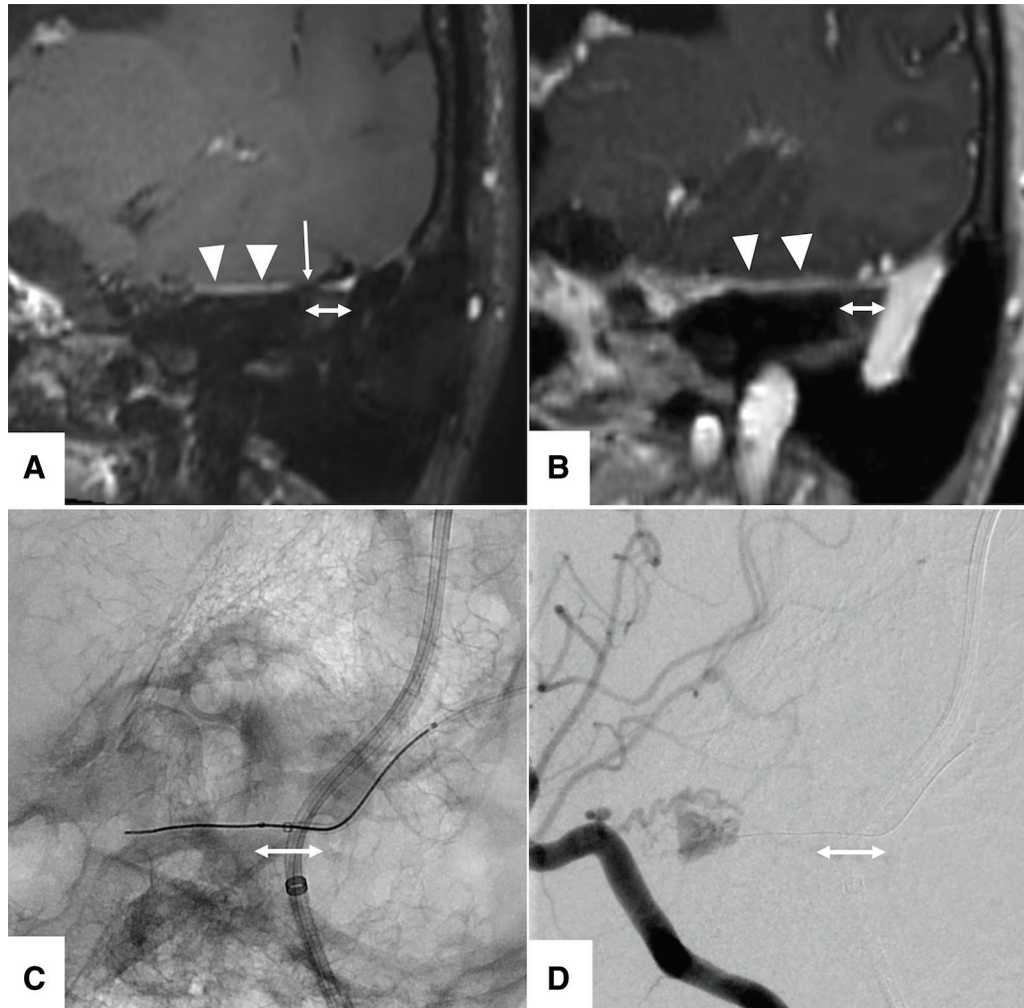


**Fig. 4** Comparison of contrast-enhanced MRI and DSA images for details of SPS. (**A** and **B**) The reconstructed oblique images of **Fig. 2C** and **2D** at the same angle in which the SPS is visible along the long axis. In these contrast-enhanced MRI images, the arrowhead shows enhanced SPS, and the thin arrow shows the area of decreased signal in contrast-enhanced 3D-T1 SPACE images. (**C** and **D**) The lateral view of the digital angiography and DSA when the micro guide-wire advanced to varix, but the microcatheter could not easily advance. As measured by the distance to the inner edge of the transverse sinus in each image, the tip of the microcatheter was precisely matched to the low signal area in the contrast-enhanced MRI. The double-headed arrows in each image indicate equal distance. SPACE: sampling perfection with application optimized contrasts using different flip angle evolutions; SPS: superior petrosal sinus

through it relatively easily. As shown in **Fig. 4**, the tip of the microcatheter at that time coincided with the low-intensity area in the 3D-T1 SPACE. Resistance to the catheter advancement was observed only in the low-intensity area. Therefore, based on this behavior of the device, we believed that this low-intensity area could suggest partial stenosis or tortuosity of the SPS.

Lawton et al. demonstrated good surgical outcomes by extended retrosigmoid approach in all eight SPS-DAVF patients.<sup>9</sup> However, in a report on TAE outcomes combined with craniotomy, some perioperative complications occurred in 10 of 18 patients (56%).<sup>2</sup> A report demonstrated that SPS-DAVF, a feeder by MHT from the anterior

circulation, is more likely to recur with TAE.<sup>15</sup> Because both TAE and craniotomy are highly at risk for treating SPS-DAVF, TVE is safe and definitive without ischemic risk of vasa nervorum. Therefore, preoperative sufficient evaluation, including contrast-enhanced MRI, should be performed to determine whether TVE is feasible or not.

## Conclusion

We reported a successful TVE case of SPS-DAVF with cortical venous reflux, which was assumed to have a high surgical risk for craniotomy and TAE. In addition to the contrast-enhanced 3D-T1 FFE, 3D-T1 SPACE might

provide beneficial information for endovascular therapy in the evaluation of venous sinuses, which is undetectable by standard examinations such as CTA and DSA.

## Disclosure Statement

Takashi Izumi received a research grant from KANEKA MEDIX CORP. The other authors declare no conflict of interest.

## References

- 1) Hiramatsu M, Sugiu K, Hishikawa T, et al. Results of 1940 embolizations for dural arteriovenous fistulas: Japanese Registry of Neuroendovascular Therapy (JR-NET3). *J Neurosurg* 2020; 133: 166–173.
- 2) Ng PP, Halbach VV, Quinn R, et al. Endovascular treatment for dural arteriovenous fistulae of the superior petrosal sinus. *Neurosurgery* 2003; 53: 25–32; discussion 32–33.
- 3) Shimada R, Kiyosue H, Tanoue S, et al. Superior petrosal sinus: hemodynamic features in normal and cavernous sinus dural arteriovenous fistulas. *AJNR Am J Neuroradiol* 2013; 34: 609–615.
- 4) Branco G, Takahashi A, Ezura M, et al. Dural arteriovenous shunt involving the superior petrosal sinus: presentation and treatment by transvenous embolisation via the occipital and transverse sinuses. *Neuroradiology* 1997; 39: 67–70.
- 5) Hou K, Lv X, Qu L, et al. Endovascular treatment for dural arteriovenous fistulas in the petroclival region. *Int J Med Sci* 2020; 17: 3020–3030.
- 6) Hosoo H, Tsuruta W, Nakai Y, et al. The visualization methods of occluded dural sinus for safe transvenous embolization of dural AVFs. *World Neurosurg* 2019; 127: e337–e345.
- 7) Awad IA, Little JR, Akarawi WP, et al. Intracranial dural arteriovenous malformations: factors predisposing to an aggressive neurological course. *J Neurosurg* 1990; 72: 839–850.
- 8) Satoh K, Satomi J, Nakajima N, et al. Cerebellar hemorrhage caused by dural arteriovenous fistula: a review of five cases. *J Neurosurg* 2001; 94: 422–426.
- 9) Lawton MT, Sanchez-Mejia RO, Pham D, et al. Tentorial dural arteriovenous fistulae: operative strategies and microsurgical results for six types. *Neurosurgery* 2008; 62: 110–124; discussion 124–125.
- 10) Takahashi S, Sakuma I, Tomura N, et al. Transvenous embolization of dural arteriovenous fistula of the cavernous sinus. Fistulous points and route of catheterization. *Interv Neuroradiol* 2004; 10 Suppl 1: 85–92.
- 11) Tanoue S, Kiyosue H, Okahara M, et al. Para-cavernous sinus venous structures: anatomic variations and pathologic conditions evaluated on fat-suppressed 3D fast gradient-echo MR images. *AJNR Am J Neuroradiol* 2006; 27: 1083–1089.
- 12) Raghuram K, Durgam A, Sartin S. Assessment of the inferior petrosal sinus on T1-weighted contrast-enhanced magnetic resonance imaging. *J Clin Imaging Sci* 2018; 8: 22.
- 13) Sommer NN, Pons Lucas R, Coppenrath E, et al. Contrast-enhanced modified 3D T1-weighted TSE black-blood imaging can improve detection of infectious and neoplastic meningitis. *Eur Radiol* 2020; 30: 866–876.
- 14) Niu PP, Yu Y, Guo ZN, et al. Diagnosis of non-acute cerebral venous thrombosis with 3D T1-weighted black blood sequence at 3T. *J Neurol Sci* 2016; 367: 46–50.
- 15) Stapleton CJ, Patel AP, Walcott BP, et al. Surgical management of superior petrosal sinus dural arteriovenous fistulae with dominant internal carotid artery supply. *Interv Neuroradiol* 2018; 24: 331–338.